



Cellulose nanocrystals from sugarcane bagasse and its graft with GMA: Synthesis, characterization, and biocompatibility assessment

Abdelrahman Barakat¹, Alaa Fahmy¹, Shahira H. EL-Moslamy², Esmail M. El-Fakharany³, Elbadawy A. Kamoun^{4,5*}, Mohamed Bassyouni¹

¹Chemistry Department, Faculty of Science, Al-Azhar University, Cairo, Egypt.

²Bioprocess Development Department, Genetic Engineering and Biotechnology Research Institute (GEBRI), City of Scientific Research and Technological Applications (SRTA-City), New Borg Al-Arab City 21934, Alexandria, Egypt.

³Protein Research Department, Genetic Engineering and Biotechnology Research Institute (GEBRI), City of Scientific Research and Technological Applications (SRTA-City), New Borg Al-Arab City 21934, Alexandria, Egypt.

⁴Polymeric Materials Research Department, Advanced Technology and New Materials Research Institute (ATNMRI), City of Scientific Research and Technological Applications (SRTA-City), New Borg Al-Arab City 21934, Alexandria, Egypt.

⁵Nanotechnology Research Center (NTRC), The British University in Egypt (BUE), El-Sherouk City, Cairo 11837, Egypt.

ARTICLE INFO

Received on: 02/09/2020
Accepted on: 27/10/2020
Available online: 05/02/2021

Key words:

Cellulose nanocrystals, extraction, CNC-g-GMA, *in vitro* bioevaluation tests.

ABSTRACT

This work presents the preparation of cellulose nanocrystals (CNCs) from sugarcane bagasse via acid hydrolysis of bleached pulp. Crystallinity and size of CNCs were characterized by XRD and zetasizer at 77% and 260 nm, respectively. CNCs were graft copolymerized in an aqueous suspension by a redox-initiated free radical method using cerium ammonium nitrate (CAN) as the initiator. Glycidyl methacrylate (GMA) was grafted onto CNCs to improve its physicochemical properties and biological activity. The parameters affecting the grafting of CNCs-g-GMA, e.g., GMA and CAN concentrations and grafting time were studied. The results revealed that high grafting yield (~180%) was obtained by increasing GMA and middle concentration of the CAN initiator (2 mmol/g). The grafting yield (%) of CNCs-g-GMA for all grafting conditions was calculated gravimetrically, while CNCs-g-GMA was characterized by FTIR, scanning electron microscope, and thermal gravimetric analysis analyses. Antimicrobial activity of CNCs and CNCs-g-GMA was assessed *in vitro* against human Gram +ve and -ve bacteria and against *Candida albicans* fungus. 2.5 g l⁻¹ of CNCs-g-GMA copolymer showed the highest antimicrobial activity, due to its significant ability to kill ~80% of *Staphylococcus aureus*, 71.4% of *Salmonella typhimurium*, and 70% of *Klebsiella pneumoniae*. Also, CNCs and CNCs-g-GMA exhibited clinically accepted cell viability (%) with almost 90%–100% versus HDF and WI38 human normal cell lines.

INTRODUCTION

Cellulose is among the most naturally occurring and biodegradable polymers (Salas *et al.*, 2014). Many natural sources of cellulose include wood, cotton, rice straw, and sugarcane

bagasse (SCB) (Li *et al.*, 2012). Sugarcane is a green substance that is commonly used in the sugar industry, while SCB is the remains of cane stalks left over after the sugarcane juice has been crushed and extracted (Mdletshe, 2019). Bagasse is the byproduct of the sugarcane plant produced after the extraction of sucrose. This has a high proportion of cellulose, which can easily be separated by pulping from the other components, namely lignins and hemicelluloses (Mokhena *et al.*, 2017). Bagasse provides a perfect opportunity to manufacture value-added goods from such a cheap source of biomass (Zanin *et al.*, 2000). SCB produces 40%–50% crystalline cellulose. Hemicellulose is an amorphous polymer consisting mainly of glucose, mannose, galactose, xylose, arabinose, and rhamnose in addition to other

*Corresponding Author

Elbadawy A. Kamoun, Polymeric Materials Research Department, Advanced Technology and New Materials Research Institute (ATNMRI), City of Scientific Research and Technological Applications (SRTA-City), New Borg Al-Arab City 21934, Alexandria, Egypt.
E-mail: e-b.kamoun@tu-bs.de, badawykamoun@yahoo.com

elements in SCB as much as 25%–35%, while the rest is mainly lignin 18%–24% (Mokhena *et al.*, 2017). Cellulose are a natural linear anhydroglucose units connected by glycoside bonds to one and four carbon atoms (Kadla and Gilbert, 2000). Cellulose has excellent stability, low density, and good biodegradability. There are several forms of cellulose (I, II, III, IV and V), and it is common to find cellulose types I and II in nature (Sofla *et al.*, 2016). Cellulose type I has top mechanical characteristics and a parallel chain orientation, while cellulose type II has an antiparallel chain (Klemm *et al.*, 2005). Nanometer-sized cellulose or nanocellulose range from 10 to 350 nm. Nanocellulose has a greater surface area than cellulose, and nanocellulose is one of the alternative ways for making cellulose easier to modify (Wulandari *et al.*, 2016). Also, nanocellulose have an high aspect ratio, strong mechanical stability, low thermal expansion, low toxicity, and many –OH groups at surface that can be easily functionalized chemically (Lin *et al.*, 2012). In recent decades, cellulose modification has received considerable attention with the goal of modifying properties, such as its morphology and compatibility with other polymer materials (Mais *et al.*, 2000). A wide variety of applications are anticipated to be identified for grafted cellulose.

However, biocomposites are primarily studied in two areas; i.e., as specific building materials and for a variety of biomedical applications (Carlmark *et al.*, 2012). Cellulose might be grafted with polymers as follows: (1) adding developed polymer chains to the cellulose backbone (grafting onto the backbone), (2) developing new polymer chains from radical sites on the backbone (grafting from), or (3) inserting vinyl groups into the cellulose and copolymerizing the resulting macromonomer with a small molecular weight co-monomer (grafting through) (O'dian, 2004). Graft copolymerization of vinyl monomers, e.g., methacrylate group, onto cellulose can introduce versatile features and enrich the field of potential application of grafted cellulose by the addition of side chains. Recently, different initiator systems have been utilized to initiate the graft copolymerization of cellulose. Initiators, such as cerium ammonium nitrate (CAN), potassium persulfate, and ammonium persulfate, produce free radicals onto grafted cellulose (Joshi and Sinha, 2006). A free radical copolymerization initiated by ammonium cerium (IV) nitrate ((NH₄)₂Ce(NO₃)₆, (CAN) was chosen for the experiments, as it has been thoroughly tested and is a selective method for grafting of polysaccharides toward the vinyl monomer (O'Connell *et al.*, 2006). Cellulose graft copolymers were strongly tested, involving the growth of polymer grafts directly from the cellulose backbone in a conventional free radical polymerization process (Kang *et al.*, 2015). Glycidyl methacrylate (GMA) was chosen for the grafting reaction of cellulose based on the fact that GMA appendages endow cellulose with new properties and due to the surface GMA network formation that acts like a molecular sponge. GMA-g-cellulose was defined as a multitasking material as it found applications in relatively diverse fields (Vismara *et al.*, 2012). Nanocellulose grafted with GMA improved the capability of CNCs to bind water-soluble antibiotics (e.g., tetracycline and doxorubicin), and bind nonionized hydrophobic anticancer agents (Jackson *et al.*, 2011). Also, graft copolymerization with GMA could act in synergy with holding drugs and as reinforcement of the hydrogel matrix (Vismara *et al.*, 2012), while polysaccharide

materials derivatized with GMA were loaded with antibiotics which have topic antibacterial activity (Vismara *et al.*, 2009).

This work aims to prepare cellulose nanocrystals (CNCs) extracted from SCB. CNCs were produced by the acid hydrolysis process. CNCs were characterized for verifying their nanoscales. CNCs were proposed as suitable reinforcing agents in the fabrication of bionanocomposites for different applications. The obtained CNCs were modified by graft copolymerization with GMA to add new functionality epoxide groups. A free radical copolymerization initiated by IV nitrate was utilized for grafting GMA onto cellulose chains. Surface topography, chemical composition, crystallinity, and thermal stability for the CNCs-g-GMA were characterized by scanning electron microscope (SEM), FTIR, XRD, and thermal gravimetric analysis (TGA) analyses, respectively. In addition to bioevaluation assessments, anti-microbial activity and cytotoxicity assay were investigated and discussed in detail.

MATERIALS AND METHODS

Materials

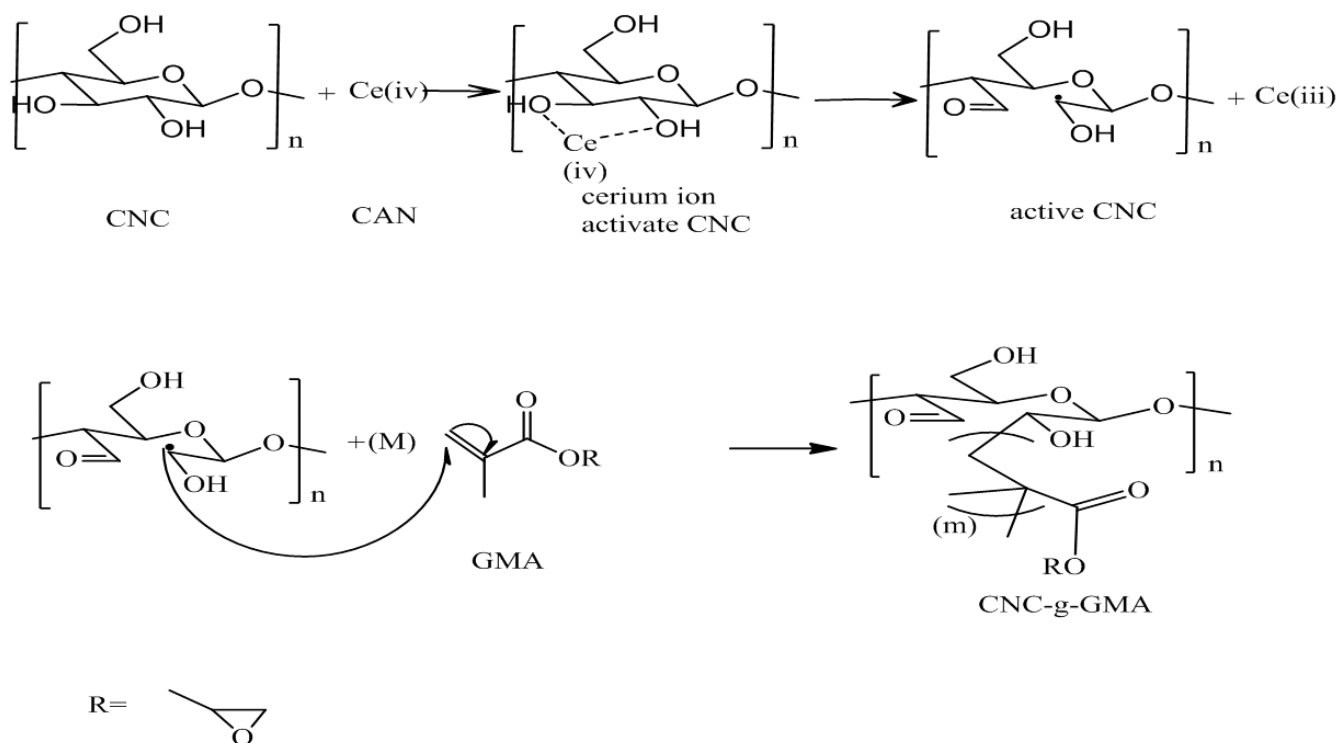
SCB (agro-waste mixtures of different types of sugarcane) was provided from Egyptian Sugar and Integrated Industries Company. Sodium chlorite (NaClO₂), glacial acetic acid, sodium hydroxide, and sulfuric acid (85%) were obtained from El-Nasr Co. for Intermediate Chemicals, Egypt. Cellulose dialysis membrane is a semi-permeable membrane, and cellulose acetate, GMA, nitric acid, and IV nitrate (CAN) were purchased from Sigma-Aldrich, Germany. Acetone, THF, methanol, and nitric acid were purchased from Fluka, Germany.

Methods of isolation of cellulose from SCB

Five grams of dried SCB were suspended in 125 ml distilled water for bleaching in a 250 ml conical flask, then 0.5 g of sodium chlorite was added to the bagasse colloidal and glacial acetic acid was added drop by drop to adjust pH < 4.0. The mixture was heated in a water bath at 70°C for 1 hour. The bleaching process was repeated at hourly intervals. Four hours of extraction was sufficient for the product to become white. The contents of the flask were filtered and the bleached cellulose fibers were washed with distilled water until the mixture neutralized. The bleached SCB was air-dried. Three grams of dry bleached bagasse was torn into small pieces in a beaker and kept in a water bath at 20°C. Afterward, 50 ml of 17.5% (w/w) of NaOH was added with continuous stirring for 45 minutes. Then, 100 ml of distilled water was added to the mixture and it was harshly stirred for further 30 minutes. The produced cellulose suspension was filtered and washed with 500 ml distilled water then with 100 ml of 10% acetic acid. The washing with distilled water was repeated until the cellulose became neutral. The pure cellulose was air-dried and preserved in a brown bag.

Synthesis of CNCs

The hydrolysis method was employed for preparing the nanocellulose as explained by Ferreira *et al.* (2018). One gram of cellulose only was added to 40 ml of 65% (w/w) sulfuric acid. The suspension was warmed to 50°C and vigorously stirred for 40 minutes. For stopping the reaction, 100 ml of distilled water



Scheme 1. Reaction mechanisms of grafting of CNCs with GMA using cerium-initiated copolymerization.

was added, and then centrifuged at 6,000 rpm for 15 minutes. The mixture was washed with distilled water and centrifuged five times until pH was >5. The nanocellulose suspension was dialyzed against distilled water for 5 days and then stored at 4°C. Dried nanocellulose was obtained by lyophilization for 48 hours.

Synthesis of CNCs-g-GMA copolymer

GMA was grafted onto CNCs using the method described by [Littunen *et al.* \(2011\)](#). Briefly, the concentration of CNCs/water suspension was reduced to 0.1 (wt. %) and the pH value was fixed to 2 using nitric acid of 0.3 M. For 10 minutes, nitrogen gas was bubbled through the mixture with continuous stirring for 30 minutes, followed by addition of the CAN initiator in various concentrations (1, 2, and 4 ml mol/g) with continuous stirring for further 15 minutes at 40°C. 20, 40, and 80 ml mol/g of GMA were enlarged dropwise for 30 minutes, with gentle stirring for further 30, 60, and 120 minutes, respectively ([Scheme 1](#)). A series of CAN initiator concentrations were used for 1, 2, or 4 ml mol/g of dry CNCs. The GMA series were also studied for 20, 40, or 80 ml mol/g of dry CNCs. The mixture was centrifuged at 3,000 rpm for 30 minutes and the precipitate was rinsed with distilled water for removing the traces, non-reactants of initiator, and acid. Afterward, acetone and THF were utilized for washing the obtained residue to withdraw the homopolymer from the graft copolymer. The washing solution was mixed with a non-solvent (e.g., methanol) and the precipitated homopolymer was centrifuged. Furthermore, for drying the grafted CNC-g-GMA copolymer and homopolymer, the samples were kept overnight at room temperature ([Bloch, 2003](#)).

Instrumental characterization of CNCs and CNCs-g-GMA copolymer

Particle size analyzer

The particle size of the CNCs was verified by the particle size of the analyzer with a Beckman Coulter Delsa™ Nano, Japan. The CNCs were dispersed in distilled water and introduced into the cuvette. The measurement was carried out in the range of measurement from 10 to 4,000 nm at room temperature.

Scanning electron microscope (SEM)

The morphological measurements of CNCs and CNCs-g-GMA copolymer were carried out on SEM with 10 kV voltage (type: JEOL, JSM-6360LA, Tokyo, Japan) with a magnification of 1,000x, 3,000x, and 5,000x.

FTIR

The chemical structure of CNCs and grafting reaction of CNCs-g-GMA copolymer were verified by Fourier transform infrared spectroscopy (Shimadzu FTIR-8400 S, Kyoto, Japan). The data were analyzed at 25°C, in the spectral range from 4,000 to 400 cm^{-1} , and 16 scans per sample cycle.

XRD

The crystallinity of probes was investigated using X-ray diffraction (PW 1,830 Diffractometer, Japan). Cu K_α with a step size of 0.02 was employed for this measurement and the crystallinity index (C_i) was estimated utilizing equation (1) ([Park *et al.*, 2010](#)), by determining the crystalline region of I_{200} and the amorphous region (I_a) as follows:

$$C_i = \frac{I_{200} - I_a}{I_{200}} \times 100\% \quad (1)$$

Thermal gravimetric analysis (TGA)

The TGA of CNCs and CNCs-g-GMA was measured using the TGA instrument (Shimadzu TGA-50, Japan). 20°C/minutes was the heating rate under flow for N₂ up to 600°C.

Grafting efficiency

The gravimetric calculation was used in order to assess the grafting process of CNCs-g-GMA, where CNCs-g-GMA was weighed and the results were employed to determine the graft yield using the given equation (2)

$$\text{Graft yield} = \frac{W_g}{W_c} \times 100\% \quad (2)$$

where W_g is the obtained mass of CNCs-g-GMA and W_c is the initial mass of CNCs.

Antimicrobial properties of CNCs and CNCs-g-GMA copolymer

In this work, different human pathogens, such as *Escherichia coli* (-ve), *Klebsiella pneumonia* (-ve), *Staphylococcus aureus* (+ve), *Salmonella typhimurium* (+ve), and *Candida albicans*, were tested to detect the antimicrobial activities for the synthesized CNCs (1, 2, and 4 g l⁻¹) and the grafted CNCs-g-GMA copolymer (1, 2, and 4 g l⁻¹) separately. Furthermore, the inhibitory effects of different dilutions of CNCs-g-GMA (3.5, 3, 2.5, and 1.5 g l⁻¹) against the tested human pathogens were checked and mathematically estimated using turbidity measurements according to Koch's method (Goy *et al.*, 2016). First, these pathogens were cultured using nutrient broth (2 g/l) at 37°C ± 2°C for 24 hours to prepare the stock cultures. Subsequently, these cultures were diluted with sterilized nutrient broth to get an optical density of 0.08 at 600 nm. Afterward, the CNCs and CNCs-g-GMA solutions were added separately to these cultures except the control (untreated sample) which contained the culture only. These solutions were then incubated at 200 rpm, at 37°C ± 2°C for 18 hours. After the incubation period, the microbial growth was estimated via spectrophotometer at 600 nm to calculate the antimicrobial effectiveness. Since the reduction of the microbial growth quantified as a function of the tested polymer, the antimicrobial efficiency can be mathematically determined employing the maximum absorbance measurements in each case (turbidity data). Three replicas were measured for each sample and the final data were exposed to statistical evaluation by one-way analysis alteration ($p \leq 0.05$) utilizing Minitab 17 software. In this case, the antimicrobial efficiency can be established as a relationship between the maximum microbial growth (stationary phase) with and without the tested toxins which coded as G_p and G_c, respectively via Eq. 3 (Da Silva *et al.*, 2010).

$$Ac \rightarrow \left(\frac{dG_c}{dt} \right)_{max}^{Control} = 0 \quad \text{and} \quad Ac \rightarrow \left(\frac{dG_p}{dt} \right)_{max}^{Polymer} = 0$$

$$Af(\%) = \left[\frac{Ac - Ap}{Ac} \right] \times 100 \quad (3)$$

where A_c and A_p are the maximum absorbances at 600 nm for the control and treated cultures, respectively, and A_f is considered as the calculated inhibitory proportional factor.

Cytocompatibility of CNCs and CNCs-g-GMA on the viability of normal cells

The effect of CNCs and CNCs-g-GMA on the cell viability of HDF (fibroblast cells originated from human dermal tissue) and WI38 (fibroblast cells obtained from human lung tissue) normal cells was evaluated using the 3-(4,5-dimethylthiazol-2-yl)-2,5-diphenyltetrazolium bromide (MTT) cell viability procedure as previously assessed by Mosmann (1983) and El-Fakharany *et al.* (2020). In brief, HDF and WI38 cells (1.0 × 10³) were scattered in a 96-well flat bottom tissue culture sterile microplates and cultured in the DMEM media (Lonza, USA) enhanced with 10% fetal bovine serum at 37°C for 24 hours in a 5% CO₂ incubator. Then, both CNCs and CNCs-g-GMA samples were added to the cells at concentrations of 0.5, 1.0, 1.5, 2.0, 2.5, and 3.0 mg/ml and incubated at 37°C in 5% CO₂ incubator for 1, 2, and 3 days. The cells were rinsed three times with fresh media after incubation to remove the samples and dead cells. Then, about 200 μl of MTT solution at a concentration of 0.5 mg/ml was inserted into each well and developed for 3 hours at 37°C in the 5% CO₂ incubator. The formed formazan crystals were dissolved in 200 μl/well of DMSO and the optical density was measured at 630 nm and subtracted from measuring at 570 nm using reader a microplate ELISA reader. All tests were carried out in triplicates and the relative cell viability (%) evaluated to control wells containing cells without treatment was analyzed by applying the formula: (X) test/ (Y) control × 100%.

RESULTS AND DISCUSSION

Particle size measurement of CNCs

The dispersed CNCs/water mixture solution was employed to verify the actual particle size of CNCs, as shown in Figure S1 (supplementary materials), using the duplicated particle size analyzer. The dispersed CNCs show a narrow and sharp peak at around 156–370 nm diameter. This result refers to the prepared CNCs which belong to the nanoscale with a mean particle size of ~260 nm.

Grafting yield (%) optimization of CNCs-g-GMA copolymer

Different degrees of grafting yields of CNCs-g-GMA were obtained with variations in grafting reaction conditions, e.g., GMA content, CAN initiator concentration, grafting time, and grafting temperature. Table 1 displays the obtained graft yield of CNCs-g-GMA as a function of grafting conditions.

As shown in Figure 1a, the grafting yield (%) of the resultant CNCs-g-GMA increases clearly to be 115%, 180%, and 170% for GMA ratios of 20, 40, and 80 ml mol/g of CNC, respectively. This is owing to the increasing portion of GMA results in increasing the vinyl groups in CNCs-g-GMA, which facilitates the copolymerization reaction and accompanies the increase in the grafting yield % (Sun *et al.*, 2018). Thus, 40 ml mol was chosen as the optimum GMA ratio, due to its own high grafting yield (%) (i.e., 180%). In the same manner, the influence of the CAN initiator concentrations in the range of 1, 2, and 4 ml mol were studied

Table 1. Grafting yield optimization of CNCs-g-GMA copolymer.

Grafting conditions	GMA (ml mol/g)	CAN (ml mol/g)	Time (minute)	temperature (°C)	Grafting yield (G _y)
GMA concentration	20	2	60	40	115
	40	2	60	40	180 ^a
	80	2	60	40	170
CAN concentration	40	1	60	40	120
	40	2	60	40	180 ^a
	40	4	60	40	150
Time of grafting	40	2	30	40	120
	40	2	60	40	180 ^a
	40	2	120	40	135
Temperature of grafting	40	2	60	25	110
	40	2	60	40	180 ^a
	40	2	60	60	115

^aThe highest value of G_y %.

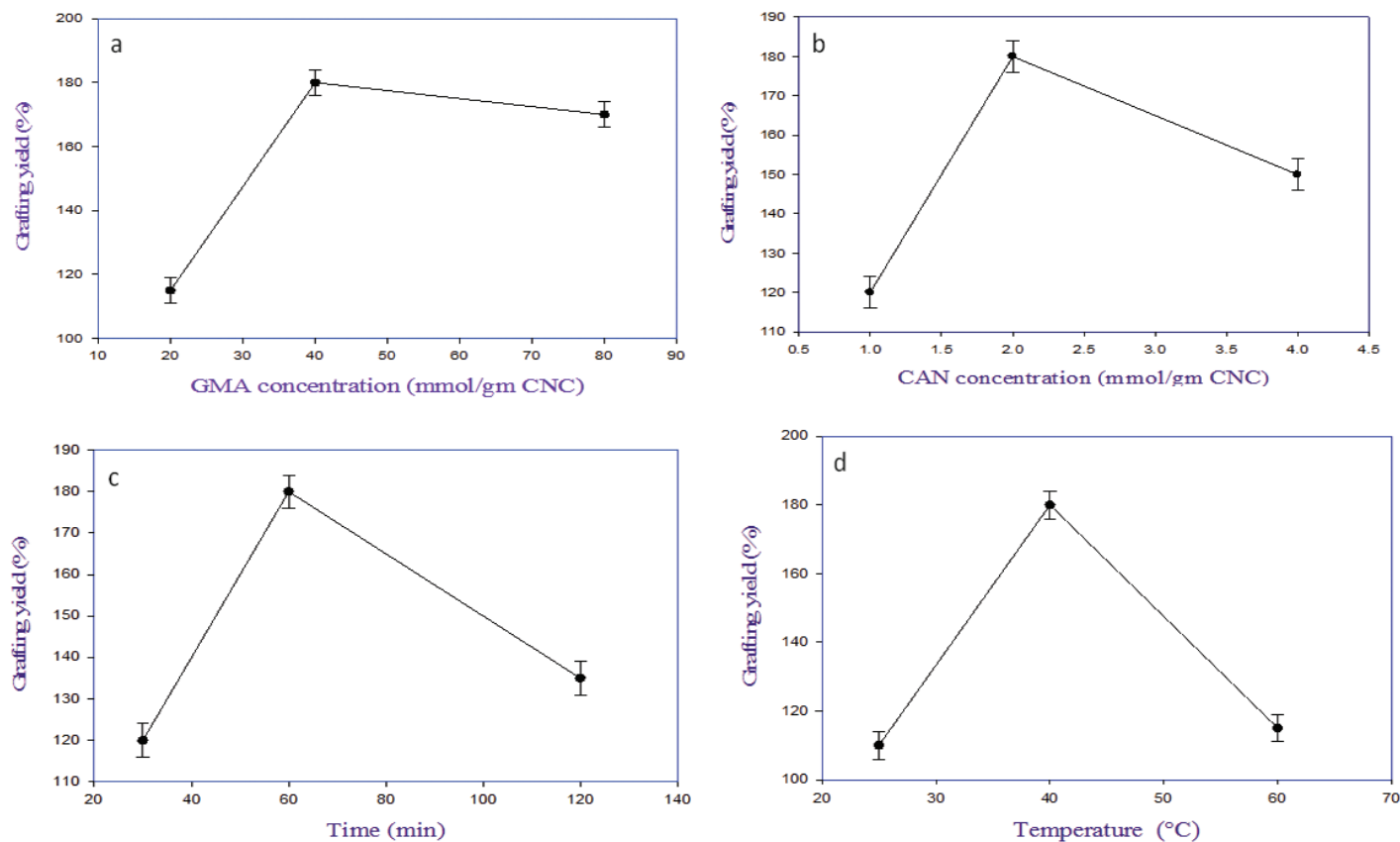


Figure 1. Grafting yield (%) of CNCs–GMA copolymer. Effect of (a) GMA monomer concentration, (b) CAN initiator concentration, (c) grafting time, and (d) grafting temperature on grafting yield (%) of CNC-g-GMA copolymer.

based on the resultant graft yield of CNCs-g-GMA copolymer (Table 1 and Fig. 1b). It is noted that the grafting yield increases to 120%, 180%, and 150% with CAN initiator concentrations of 1, 2, and 4 ml mol, respectively. It could be ascribed to the high concentration of CAN initiator >2 ml mol which might terminate the reaction of the grafting process (Fig. 1b) (Tosh and Routray, 2014). Thus, the CAN initiator concentration of 2 ml mol was selected as an optimum condition for a further grafting reaction. On the other hand, the influence of the grafting time was in the

range of 30, 60, and 120 minutes on the resultant grafting yield of CNCs-g-GMA copolymer, while the other grafting conditions were kept constant (Table 1 and Fig. 1c). It is clear that the grafting yield of the CNCs-g-GMA copolymer is dramatically increased from 120% to 180% after prolonging the grafting time from 30 to 60 minutes. However, the grafting yield decreased clearly to 135% as the grafting time increased to 120 minutes. Thus, 60 minutes as grafting time was chosen as the highest grafting yield of CNCs-g-GMA copolymer.

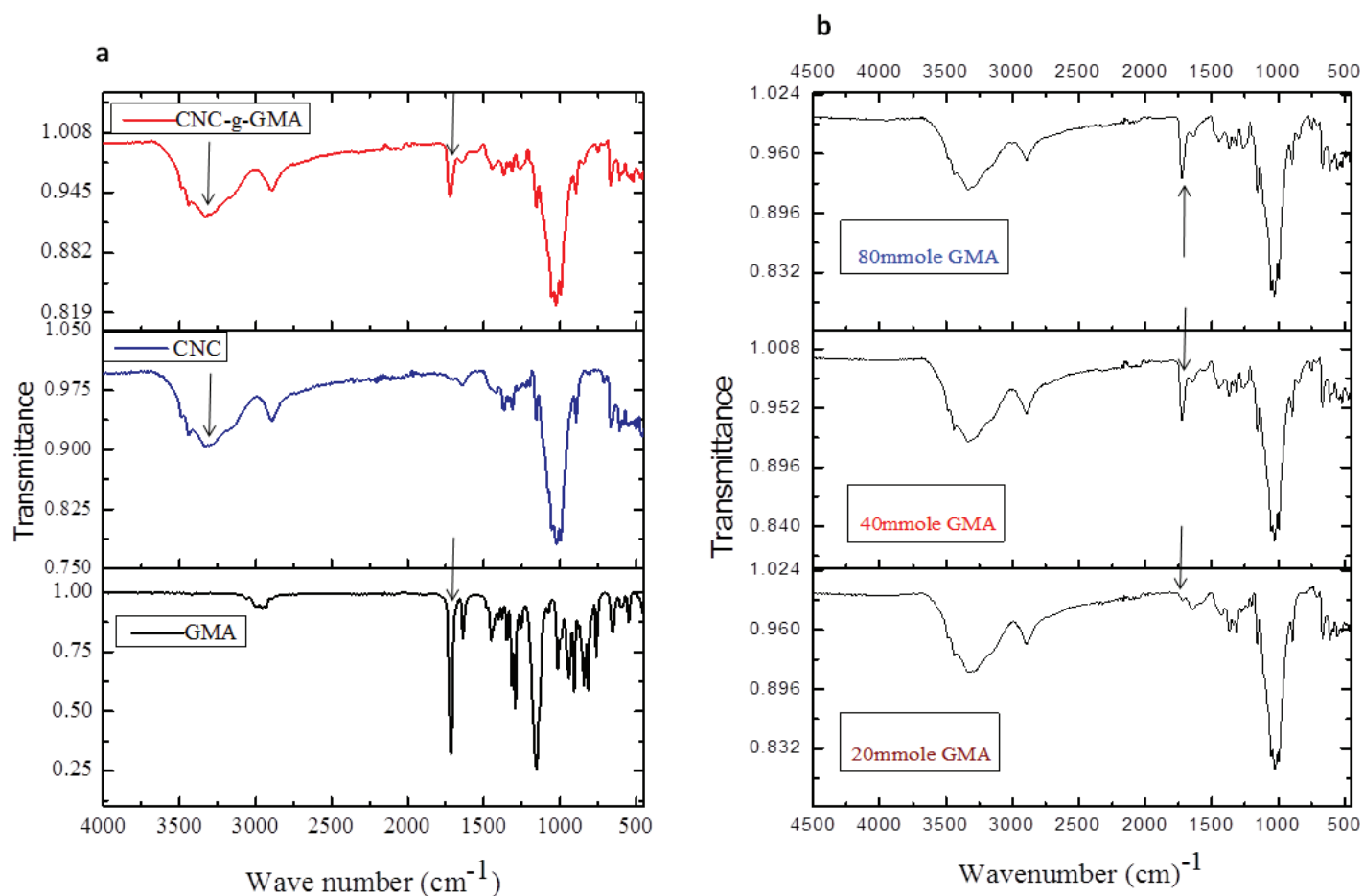


Figure 2. FTIR spectra of CNCs-g-GMA copolymer. (a) IR spectra of CNCs, GMA, and CNCs-g-GMA, and (b) as function of GMA monomer concentrations (20, 40, and 80 mmol/g of CNCs).

Likely, increasing the grafting temperature from 25°C to 40°C resulted in a significant increase of grafting yield from 110% to 180%, respectively (Fig. 1d). Notably, the grafting yield decreased to 115%, when the temperature of the grafting reaction was increased to 60°C. The reason might be referred to the decomposition of the CAN initiator at a high grafting temperature (i.e., 60°C) (Fig. S2, supplementary).

FTIR spectra of CNCs and CNCs-g-GMA copolymers

The prepared CNCs, GMA, and CNCs-g-GMA copolymers were characterized by the FTIR, as shown in Figure 2a. As can be seen, both CNCs and CNCs-g-GMA spectra provided the absorption peaks at ν 3,451 cm⁻¹ and 2,899 cm⁻¹, respectively, and were assigned to the O-H and C-H stretching vibrations, respectively. However, the peak C-O vibrations contained in the polysaccharide rings of cellulose is observed at ν 1,377 cm⁻¹, while the vibration of C-O-C in pyranose ring is indicated by the absorption peak at 1,055 cm⁻¹ (Mandal and Chakrabarty, 2011; Purwanti *et al.*, 2015). CNCs-g-GMA spectrum also showed a new and strong absorption band at ν 1,720 cm⁻¹ as a characteristic ester carbonyl group, as found in the GMA spectrum. Characteristic C-H stretching peaks (symmetric and asymmetric) were also detected in the wavenumber range of ν 2,960–2,850 cm⁻¹. In addition, a medium strength absorption peak at ν 840 cm⁻¹ characterized for an epoxy group was detected in the spectra of GMA and CNCs-g-

GMA (Hase, 1995). Interestingly, the low grafting yield (%) values exhibited significantly low intensities at ν 1,720 cm⁻¹ as observed in CNCs-g-GMA copolymer with the low concentration of GMA (20 ml mol/g), and it resulted in a very low grafting yield (%) accompanying low intensity at ν 1,720 cm⁻¹ (Fig. 2b).

Unexpectedly, the intensity of the feature absorption peak of ester carbonyl group at 1,720 cm⁻¹ was detected in a low intensity for low and high CAN initiator concentrations (1 and 4 ml mol) during the grafting process, while the methacrylation peak intensity was detected in a significantly high intensity with the middle CAN initiator concentration (2 ml mol) during the grafting process (Fig. 3a). Thus, the middle CAN initiator concentration (2 ml mol) was chosen as the optimized CAN initiator concentration for further grafting attempts. The intensity of ester carbonyl group of CNCs-g-GMA copolymer at ν 1,720 cm⁻¹ was raised notably with prolonging the grafting reaction time from 30 to 120 minutes at 60°C (Fig. 3b).

X-ray diffraction of CNCs and CNCs-g-GMA copolymer

The C_1 of CNCs was analyzed by the XRD pattern as shown in Figure 4. Three diffraction peaks at $2\theta = 12.2^\circ$, 20.1° , and 22° were detected with the CNCs. The C_1 for CNCs was estimated employing equation (1), where I_{200} at $2\theta = 22^\circ$ and I_a at $2\theta = 17.5^\circ$ (Wada *et al.*, 2004). This method was progressed by Segal *et al.* (1959), where the C_1 was evaluated from the ratio of

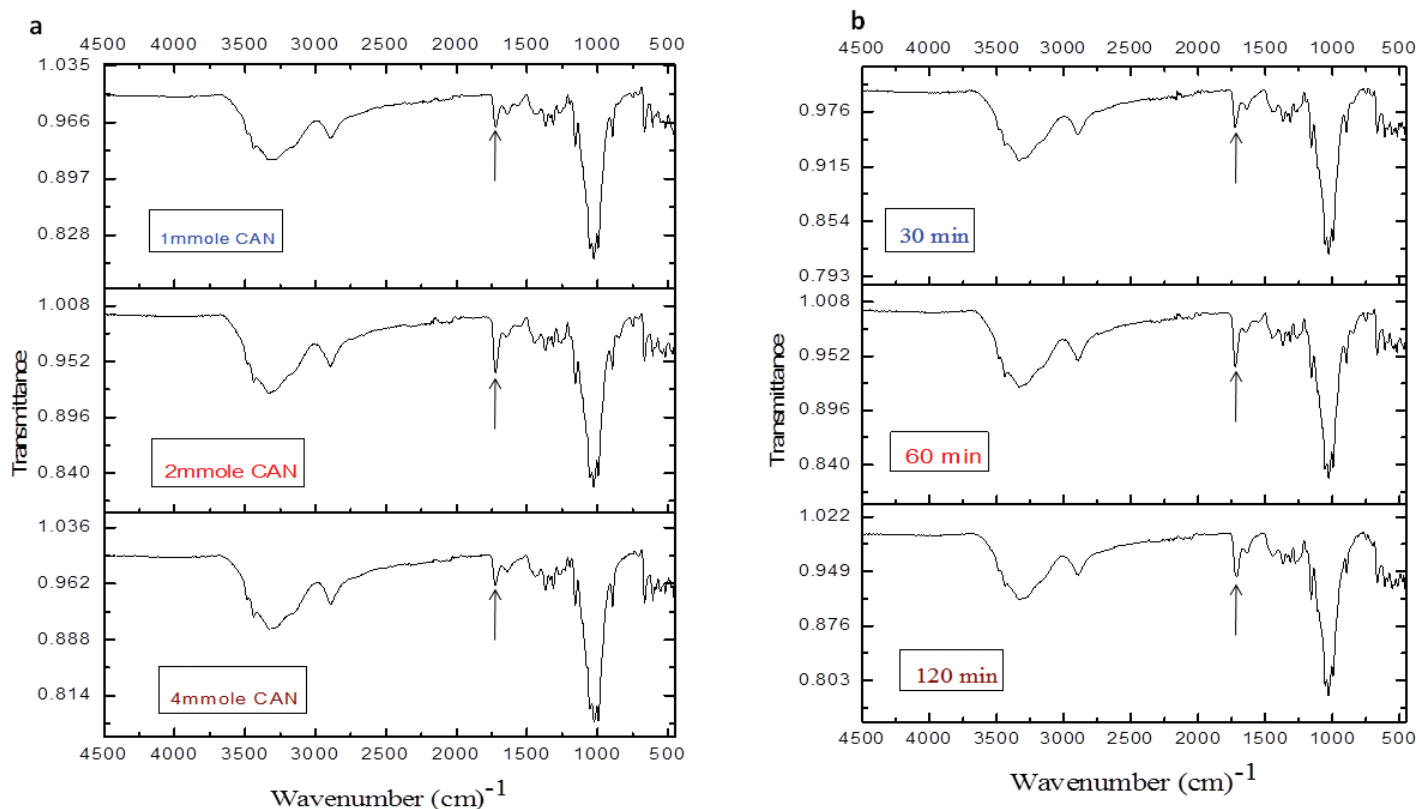


Figure 3. FTIR spectra of CNCs-g-GMA copolymer as function of (a) CAN initiator concentration (1, 2, and 4 mmol/g of CNC) and (b) grafting reaction time (30, 60, and 120 minutes) during grafting process.

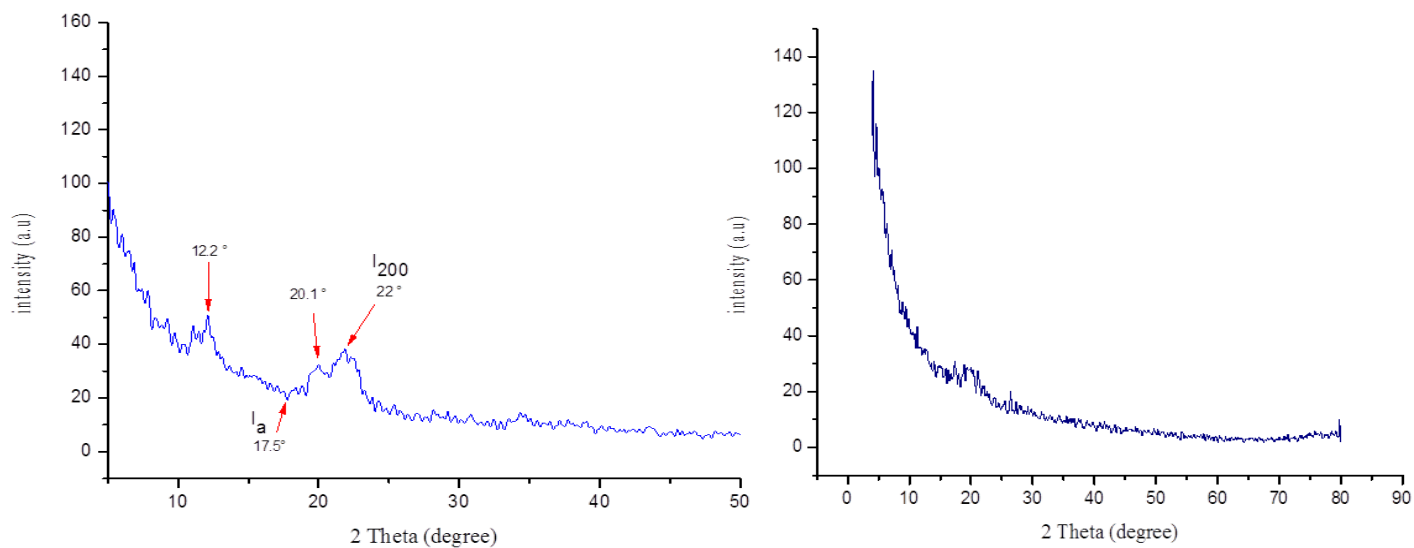


Figure 4. XRD patterns of resultant CNCs (left) and CNCs-g-GMA copolymer (right).

the height of the 002 peak (I_{002}) and the height of the minimum between the 002 and 101 peaks. The diffractograms are shown in Figure 4. The C_i for isolated CNCs from SCB is calculated ca. 77.33% as previously measured by Park *et al.* (2010).

The crystallinity of the prepared CNC-g-GMA is shown in Figure 4. The XRD pattern exhibits the loss of the crystal structure of CNC after the grafting reaction, corresponding to

the formation of CNCs-g-GMA, which resulted in changing the crystal structure of CNCs and reducing peaks intensity in the CNC-g-GMA. However, the pattern of CNCs-GMA displayed a significant increase in hydrophobic properties of CNC-g-GMA compared to CNCs (Giljean *et al.*, 2011), where the C_i of CNC-g-GMA could not be measured due to losing the intensity of crystal peak at 20~22°.

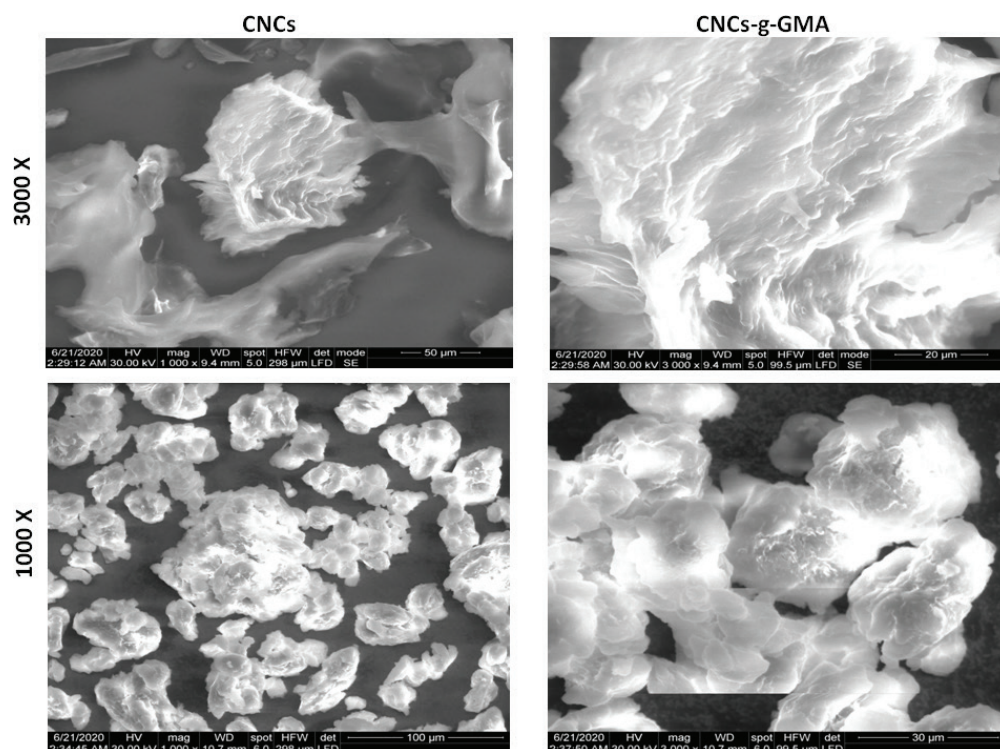


Figure 5. SEM photographs of CNCs and CNCs-g-GMA copolymer. Images were taken under original magnifications (1,000x and 3,000x) under 30 Kv.

Surface morphology of CNCs and CNCs-g-GMA copolymer

The surface morphology of CNCs and CNCs-g-GMA was investigated by SEM with 1,000x and 3,000x original magnifications under 30 kV. SEM micrographs are shown in Figure 5. The SEM images revealed that hydrolysis of cellulose produced a reduction in its raw cellulose fiber diameter (Sèbe *et al.*, 2012). Moreover, cellulose particles after hydrolysis with regard to CNCs-g-GMA showed a more irregular shape and more asymmetrical edges than CNCs. CNCs images involved fibrils that were significantly lesser than 40 nm in diameter, but thicker fibril-aggregated bundles were also observed. Comparison of these images demonstrates that the nanoscale fibrils structure is preserved during the grafting process in case CNCs-g-GMA, while the aggregation of CNCs appeared to be significantly reduced after grafting, owing to the methacrylation with regard to CNCs-g-GMA copolymer. Also, the fibrils of the CNCs-g-GMA copolymer were somewhat thicker than those of CNCs; it might be attributed to the large amounts of grafted GMA onto CNCs nanofibrils (Habibi, 2014).

TGA thermographs of CNCs and CNCs-g-GMA copolymer

TGA analysis of CNCs and CNCs-g-GMA is shown in Figure 6. As can be seen, CNCs started to thermo-decompose close to 238°C–327°C as initial decomposition stage, showing a drop in weight loss (%) to complete decomposition at almost 400°C. However, grafted CNCs exhibited a slight increase in initial decomposition stage close to 264°C–342°C, with a complete decomposition at 448°C. It means that the grafting process of CNCs might improve the thermal stability of CNCs to ca. 26°C.

Evaluation of antimicrobial efficiency of CNCs and CNCs-g-GMA

The antimicrobial effects of CNCs and CNCs-g-GMA were represented graphically using the optical density of tested pathogens, as shown in Figure 7. Since the growth of all tested human pathogens was affected by all CNCs and CNCs-g-GMA treatments, the treatment coded as F (4 gl^{-1} of CNCs-g-GMA) showed the highest antimicrobial activity and the growth of *S. aureus* (+ve) was reduced from 2.44 nm to 1.36 nm, while *S. typhimurium* (-ve) decreased from 2.39 nm to 1.35 nm (Fig. 7a). Furthermore, using turbidity data, this figure indicates that the fungal growth was also reduced using 4 gl^{-1} of CNCs-g-GMA treatment (F) from 2.71 nm to 1.62 nm, as shown in the case of tested *C. albicans*. Other than the growth of all tested fungi, pathogens could be reduced slightly by using 1, 2, and 4 gl^{-1} of CNC treatments coded as A, B, and C, respectively. Accordingly, the growth of the human pathogens can be reduced perfectly by using 4 gl^{-1} of grafted CNCs-g-GMA, compared to untreated CNCs (Fig. 7a).

Figure 7b shows the calculated inhibitory proportional factor (%) which indicated the reduction in the microbial populations concerning the tested control, especially in case of *S. aureus* (+ve), *S. typhimurium* (-ve), and *C. albicans* to 44.30%, 43.09%, and 40.29%, respectively, as a function of tested treatment coded as F (4 gl^{-1} of CNCs-g-GMA). With regard to the rest of the treatment, *E. coli* (-ve) has the highest inhibitory factor which recorded 13.62%, 17.25%, 21.24%, 28.34%, and 29.38% using A (1 gl^{-1} CNCs), B (2 gl^{-1} CNCs), C (4 gl^{-1} CNCs), D (1 gl^{-1} of CNCs-g-GMA), and E (2 gl^{-1} of CNCs-g-GMA) treatments,

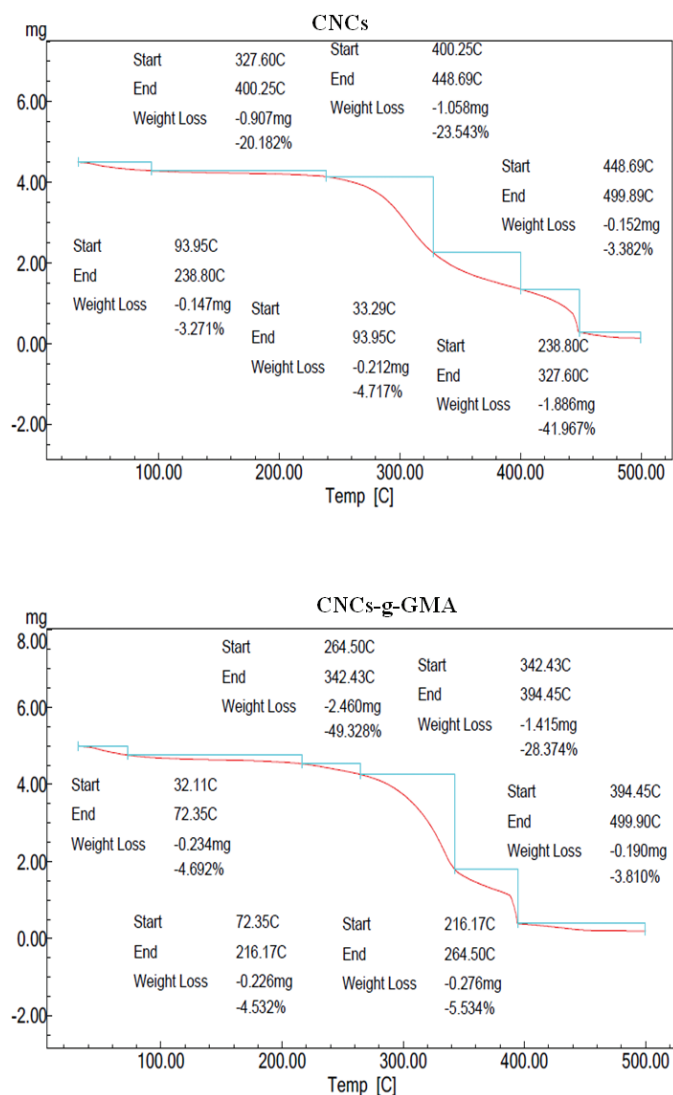


Figure 6. TGA thermograph results of CNCs and CNCs-g-GMA copolymer.

respectively. However, the lowest inhibitory factors were recorded as 5.5% with *K. pneumoniae*, followed by 7.12% of *C. albicans* and 7.8% of *S. aureus* via the treatment coded as A (1 g l^{-1} CNCs).

Furthermore, the derivative relationship for different dilutions of the tested CNCs-g-GMA copolymer (3.5, 3, 2.5, and 1.5 g l^{-1}) and the microbial growth were calculated and are graphically represented in Figure 7c. The highest antimicrobial activity recorded by calculating the inhibitory proportional factor was 79.5% against *S. aureus*, followed by *S. typhimurium* (71.4%), and *K. pneumoniae* (69.5%) using 2.5 g l^{-1} of CNCs-g-GMA copolymer (F2). In addition, 1.5 g l^{-1} of CNCs-g-GMA copolymer (F1) reduced the *C. albicans* and *E. coli* growth by 69.4, and 66.07%, respectively. The lowest inhibitory proportional factor was recorded by using 3.5 g l^{-1} of CNCs-g-GMA copolymer (F4) against all tested pathogens, especially *C. albicans* recorded at 16.34%.

In light of these findings, synthesized CNCs and its graft (i.e., CNCs-g-GMA) concentrations inhibited the growth of human pathogens whether Gram +ve, Gram -ve, or fungal cells. Conversely, the maximum activity was achieved when 2.5 g l^{-1} of

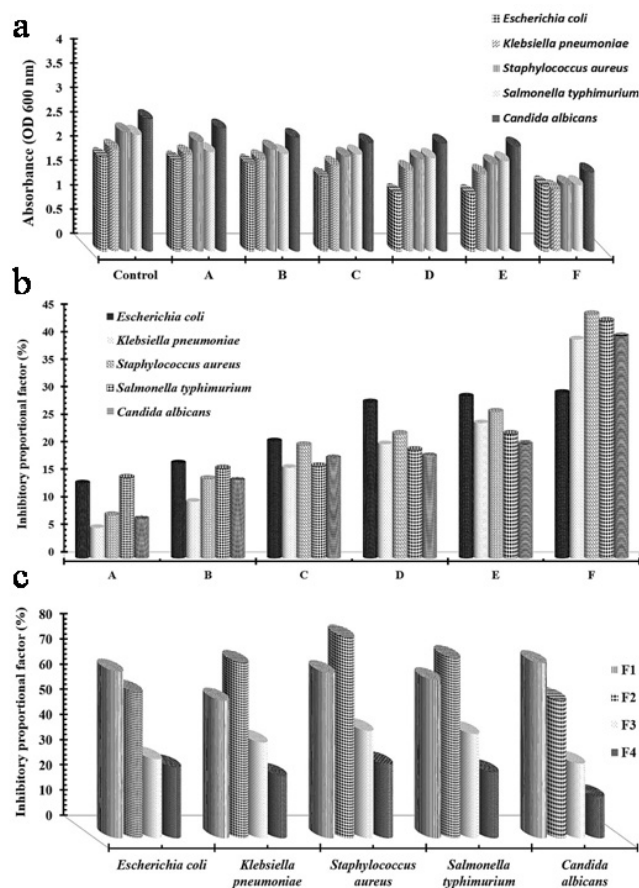


Figure 7. (a) Microbial growth absorbance at 600 nm as a function of different treatments; A, 1 g l^{-1} CNCs; B, 2 g l^{-1} of CNCs; C, 4 g l^{-1} CNCs; D, 1 g l^{-1} of CNCs-g-GMA; E, 2 g l^{-1} of CNCs-g-GMA; and F, 4 g l^{-1} of CNCs-g-GMA against different human pathogens using turbidity method after 18 hours. (b) Inhibitory proportional factor (%) according to Eq.(3) which indicated the reduction in the microbial growth in function of different CNCs, and CNCs-g-GMA treatments coded as A, 1 g l^{-1} CNCs; B, 2 g l^{-1} CNCs; C, 4 g l^{-1} CNCs; D, 1 g l^{-1} of CNCs-g-GMA; E, 2 g l^{-1} of CNCs-g-GMA; and F, 4 g l^{-1} of CNCs-g-GMA. (c) Affection of the tested concentrations of CNCs-g-GMA copolymer coded as F1: 1.5 g l^{-1} of CNCs-g-GMA; F2: 2.5 g l^{-1} of CNCs-g-GMA; F3: 3 g l^{-1} of CNCs-g-GMA; and F4: 3.5 g l^{-1} of CNCs-g-GMA against different human pathogens indicated via calculating the inhibitory proportional factor (%).

CNCs-g-GMA copolymer is added since the microbial population (*S. aureus*, *S. typhimurium*, and *K. pneumoniae*) reduced as close to 70% and 80%. The mode of action of CNCs-g-GMA copolymer might be due to its remarkable physicochemical properties that disrupted the microbial membranes by the effect of cytoplasmic membrane potentials, net surface charge, or permeability, which led to the leakage of the cellular compounds and eventually cell death (Jiang *et al.*, 2012; Liang *et al.*, 2014), since CNCs possess a special surface chemistry and excellent physical properties which make them appealing for antimicrobial applications (Panchal *et al.*, 2019).

Cytocompatibility of CNC and CNCs-g-GMA copolymer

The cytotoxicity of CNCs and CNCs-g-GMA with different concentrations (0.5, 1.0, 1.5, 2.0, 2.5, and 3.0 mg/ml) was assessed *in vitro* on human normal HDF and WI38 cell lines after 1 and 3 days of incubation (Fig. 8). As shown in Figure 8, the results revealed that CNCs has high cell viability (%) and proliferation

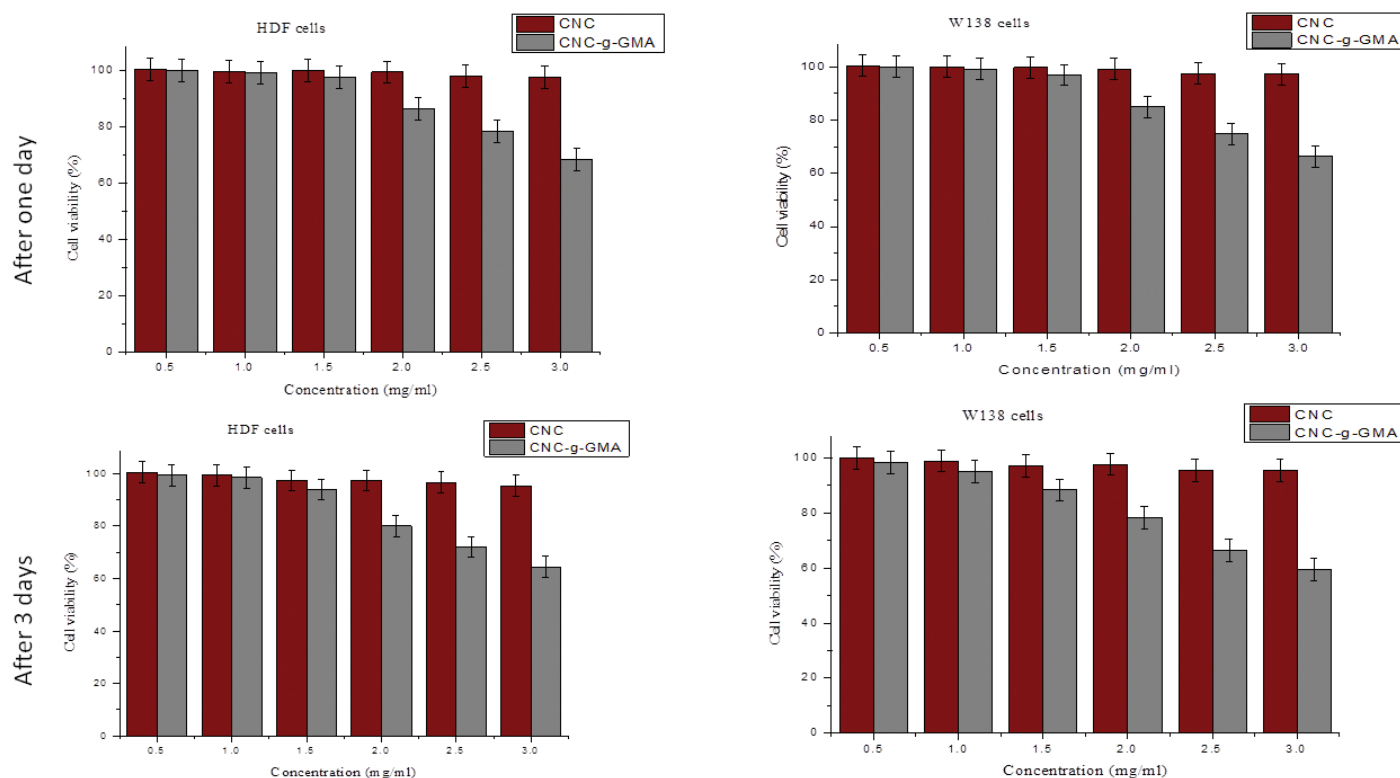


Figure 8. Influence of CNCs and CNCs-g-GMA at different concentrations (0.5, 1.0, 1.5, 2.0, 2.5, and 3.0 mg/ml) on human normal HDF and WI 38 cell lines proliferation after 1 and 3 days of incubation.

reached to 100% with all tested concentrations (0.5–3.0 mg/ml) on both days 1 and 3 of incubation. While CNCs-g-GMA copolymer with low-tested concentrations (0.5–1.5 mg/ml) shows high cell viability ranged 90%–100%, high-tested concentrations (2.0–3.0 mg/ml) exhibited a moderated and clinically accepted cell viability (%) range of 60%–80%, regardless of the type of cell lines. This observation could be attributed to CNCs-g-GMA, which might release and contain unreacted or excess of free GMA and which has cytotoxic effect on tested cell lines; thus, this cytotoxic behavior was noted only tested in high concentrations of CNCs-g-GMA in the range of 2.0–3.0 mg/ml. Accordingly, synthesized CNCs and CNCs-g-GMA possess high cytocompatibility which make them good candidates as biomaterials for biomedical applications.

CONCLUSION

SCB was used herein as a considerable source of cellulose to obtain CNCs. CNCs were synthesized by chemical purification and acid hydrolysis in two chemical steps through acid-hydrolysis to extract CNCs. The morphology of the nanocrystals was described by SEM, and the size of CNCs was detected by the particle size analyzer with an average of 156 nm. The C_1 of prepared CNCs calculated using XRD was recorded at 77.33%. CNCs were grafted in an aqueous solution employing a redox initiated free radical polymerization with GMA. The method was successful, and selective graft copolymerization with GMA monomer was dominant over homopolymerization. Both CNCs and CNC-g-GMA were characterized by FTIR which give characteristic peaks of CNCs and showed new peaks with CNC-g-GMA confirming the grafting reaction. Grafting conditions

were studied as a function in the grafting yield (%) to optimize grafting reaction conditions. The SEM investigation of CNCs-g-GMA proved a rougher surface than those of the CNCs. This form of modification might provide a quick way to boost CNCs compatibility with synthetic polymers, eliminating one barrier to solid cellulose-reinforced nanocomposites. Bioevaluation of extracted CNCs and its graft was studied against Gram +ve, Gram -ve, and fungal cells. The maximum activity was achieved with 2.5 g l⁻¹ of CNCs-g-GMA copolymer dose since the microbial population (*S. aureus*, *S. typhimurium*, and *K. pneumonia*) was reduced as close as possible to 70% and 80%, respectively. Cytotoxicity of extracted CNCs and CNCs-g-GMA were studied on HDF (fibroblast cells derived from human dermal tissue) and WI38 (fibroblast cells obtained from human lung tissue) normal cells, which showed high cell viability (%) even when using high concentrations of grafted CNCs. The grafting of CNCs with GMA might offer a simple route to enhance the compatibility and antimicrobial behavior of CNCs for using as biomaterials for versatile biomedical applications.

AUTHOR CONTRIBUTIONS

All authors made substantial contributions to conception and design, acquisition of data, or analysis and interpretation of data; took part in drafting the article or revising it critically for important intellectual content; agreed to submit to the current journal; gave final approval of the version to be published; and agree to be accountable for all aspects of the work. All the authors are eligible to be an author as per the international committee of medical journal editors (ICMJE) requirements/guidelines.

FUNDING

There is no funding to report.

CONFLICTS OF INTEREST

The authors report no financial or any other conflicts of interest in this work.

ETHICAL APPROVALS

This study does not involve experiments on animals or human subjects.

PUBLISHER'S NOTE

This journal remains neutral with regard to jurisdictional claims in published institutional affiliation.

REFERENCES

- Bloch DR. Solvents and non solvents for polymers. In Brandrup J (ed.). The Wiley database of polymer properties. John Wiley & Sons, Inc, Hoboken, NJ,
- Carlmark A, Larsson E, Malmström E. Grafting of cellulose by ring-opening polymerisation - a review. *Eur Polym J*, ;48(10):1646–59; doi:10.1016/j.eurpolymj.2012.06.013
- Da Silva LP, de Britto D, Selegim MHR, Assis OBG. *In vitro* activity of water-soluble quaternary chitosan chloride salt against *E. coli*. *World J Microbiol Biotechnol*, ;26(11):2089–92.
- El-Fakharany EM, Abu-Elreesh GM, Kamoun EA, Zakib S, Abd-EL-Haleem DA. *In vitro* assessment of the bioactivities of sericin protein extracted from a bacterial silk-like biopolymer. *RSC Adv*, 2020; 10(9):5098–107.
- Ferreira FV, Mariano M, Rabelo SC, Gouveia RF, Lona LMF. Isolation and surface modification of cellulose nanocrystals from sugarcane bagasse waste: from a micro- to a nano-scale view. *Appl Surf Sci*. 2018; 436:1113–22; doi: 10.1016/j.apsusc.2017.12.137
- Giljean S, Bigerelle M, Anselme K, Haidara H. New insights on contact angle/roughness dependence on high surface energy materials. *Appl Surf Sci*, 2011; 257(22):9631–38.
- Goy RC, Morais STB, Assis OBG. Evaluation of the antimicrobial activity of chitosan and its quaternized derivative on *E. Coli* and *S. Aureus* growth. *Rev Bras Farmacogn*, 2016; 26(1):122–27.
- Habibi Y. Key advances in the chemical modification of nanocelluloses. *Chem Soc Rev*, 2014; 43(5):1519–42.
- Hase T. Tables for organic spectrometry. Adlibris Publisher, Stockholm, Sweden, 1995.
- Jackson JK, Letchford K, Wasserman BZ, Ye L, Hamad WY, Burt HM. The use of nanocrystalline cellulose for the binding and controlled release of drugs. *Int J Nanomedicine*, 2011; 6:321.
- Jiang G, Huang W, Li L, Wang X, Pang F, Zhang Y, Wang H. Structure and properties of regenerated cellulose fibers from different technology processes. *Carbohydr Polym*, 2012; 87(3):2012–8.
- Joshi JM, Sinha VK. Graft copolymerization of 2-hydroxyethylmethacrylate onto carboxymethyl chitosan using CAN as an initiator. *Polymer*, 2006; 47(6):2198–204.
- Kadla JF, Gilbert RD. Cellulose structure: a review. *Cellulose Chem Technol*, 2000; 34(3–4):197–216.
- Kang H, Liu R, Huang Y. Graft modification of cellulose: methods, properties and applications. *Polymer*, 2015; 70:A1–16; doi:10.1016/j.polymer.2015.05.041
- Klemm D, Heublein B, Fink HP, Bohn A. Cellulose: fascinating biopolymer and sustainable raw material. *Angew Chem Int Ed*, 2005; 44(22):3358–93.
- Li W, Yue J, Liu S. Preparation of nanocrystalline cellulose via ultrasound and its reinforcement capability for poly (vinyl alcohol) composites. *Ultrason Sonochem*, 2012; 19(3):479–85.
- Liang Z, Zhu M, Yang YW, Gao H. Antimicrobial activities of polymeric quaternary ammonium salts from poly (glycidyl methacrylate) S. *Polym Adv Technol*, 2014; 25(1):117–22.
- Lin N, Huang J, Dufresne A. Preparation, properties and applications of polysaccharide nanocrystals in advanced functional nanomaterials: a review. *Nanoscale*, 2012; 4(11):3274–94.
- Littunen K, Hippi U, Johansson LS, Österberg M, Tammelin T, Laine J, Seppälä J. Free radical graft copolymerization of nanofibrillated cellulose with acrylic monomers. *Carbohydr Polym*, 2011; 84(3):1039–47; doi:10.1016/j.carbpol.2010.12.064
- Mais U, Binder WH, Knaus S, Gruber H. Synthesis and ¹³C CP MAS NMR spectroscopy of cellulose-graft-poly (N-acetyllethylenimine). *Macromol Chem Phys*, 2000; 201(16):2115–22.
- Mandal A, Chakrabarty D. Isolation of nanocellulose from waste sugarcane bagasse (SCB) and its characterization. *Carbohydr Polym*, 2011; 86(3):1291–99.
- Mdletshe GP. 2019. Extraction and characterisation of cellulose nanocrystals (CNCs) from sugarcane bagasse using ionic liquids. Durban University of Technology, Durban, South Africa.
- Mokhena TC, Mochane MJ, Motaung TE, Liganiso LZ, Thekiso OM, Songca SP. Sugarcane bagasse and cellulose polymer composites. In De Oliveira A (ed.). Sugarcane-technology and research, IntechOpen, London, UK, 2017.
- Mosmann T. Rapid colorimetric assay for cellular growth and survival: application to proliferation and cytotoxicity assays. *J Immunol Methods*, 1983; 65(1–2):55–63.
- O'Connell DW, Birkinshaw C, O'Dwyer TF. Removal of lead (II) ions from aqueous solutions using a modified cellulose adsorbent. *Adsorp Sci Technol*, 2006; 24(4):337–48.
- Odian G. Principles of polymerization. John Wiley & Sons, Hoboken, NJ, 2004.
- Panchal P, Ogunsona E, Mekonnen T. Trends in advanced functional material applications of nanocellulose. *Processes*, 2019; 7(1):10.
- Park S, Baker JO, Himmel ME, Parilla PA, Johnson DK. Cellulose crystallinity index: measurement techniques and their impact on interpreting cellulase performance. *Biotechnol Biofuels*, 2010; 3(1):10.
- Purwanti E, Wulandari WT, Rochliadi A, Bundjali B, Arcana IM. Preparation of nanocrystalline cellulose from corncob used as reinforcement in separator for lithium ion battery. In Proceedings of the Joint International Conference on Electric Vehicular Technology and Industrial, Mechanical, Electrical and Chemical Engineering (ICEVT & IMECE), IEEE, Piscataway, NJ, 2015, pp 365–69.
- Salas, C, Nypelö T, Rodriguez-Abreu C, Carrillo C, Rojas OJ. Nanocellulose properties and applications in colloids and interfaces. *Curr Opin Colloid Interface Sci*, 2014; 19(5):383–96.
- Sèbe G, Ham-Pichavant F, Ibarboure E, Koffi ALC, Tingaut P. Supramolecular structure characterization of cellulose II nanowhiskers produced by acid hydrolysis of cellulose I substrates. *Biomacromolecules*, 2012; 13(2):570–78.
- Segal L, Creely JJ, Martin Jr AE, Conrad CM. An empirical method for estimating the degree of crystallinity of native cellulose using the X-ray diffractometer. *Text Res J*, 1959; 29(10):786–94.
- Sofla MRK, Brown RJ, Tsuzuki T, Rainey TJ. A comparison of cellulose nanocrystals and cellulose nanofibres extracted from bagasse using acid and ball milling methods. *Adv Nat Sci Nanosci Nanotechnol*, 2016;7(3):35004.
- Sun L, Xueren Q, Chunyue D, Xianhui A. Integration of graft copolymerization and ring-opening reaction: a mild and effective preparation strategy for 'Clickable' cellulose fibers. *Carbohydr Polym*, 2018; 198:41–50.
- Tosh B, Chittaranjan R. Grafting of cellulose based materials: a review. *Chem Sci Rev Lett*, 2014;3(10):74–92.
- Vismara E, Melone L, Torri G. Surface functionalized cotton with glycidyl methacrylate: physico-chemical aspects and multi-tasking applications. Research project: Environment, Italy, 2012.

Vismara E, Graziani G, Montanelli G, Melone L, Torri G, *et al.* Derivatized polysaccharide material for the topic antibacterial activity. European Patent Office EP21829931B8, 2008.

Wada M, Heux L, Sugiyama J. Polymorphism of cellulose I family: reinvestigation of cellulose IVI. *Biomacromolecules*, 2004; 5(4):1385–91.

Wulandari, WT, Rochliadi A, Arcana IM. Nanocellulose Prepared by Acid Hydrolysis of Isolated Cellulose from Sugarcane Bagasse. *IOP Conf Ser Mater Sci Eng*, 2016;107:12045.

Zanin GM, Santana CC, Bon EP, Giordano RC, de Moraes FF, Andrietta SR, de Carvalho Neto CC, Macedo IC, Fo DL, Ramos LP, Fontana JD. Brazilian bioethanol program. *Appl Biochem Biotechnol*, 2000;84-86:1147-61.

How to cite this article:

Barakat A, Fahmy A, EL-Moslamy SH, El-Fakharany EM, Kamoun EA, Bassyouni M. Cellulose nanocrystals from sugarcane bagasse and its graft with GMA: Synthesis, characterization, and biocompatibility assessment. *J Appl Pharm Sci*, 2021; 11(02):114–125.